Ganymede MHD Model: Magnetospheric Context for Juno's PJ34 Flyby

Stefan Duling[1], Joachim Saur[1], George Clark[2], Frederic Allegrini[3], Thomas Greathouse[3], Randy Gladstone[3,4], William Kurth[5], John E. P. Connerney[6,7], Fran Bagenal[8], Ali H. Sulaiman[5]

[1]Institute of Geophysics and Meteorology, University of Cologne, Cologne, Germany
[2]The Johns Hopkins University Applied Physics Laboratory, Laurel, Maryland, USA
[3]Southwest Research Institute, San Antonio, Texas, USA
[4]University of Texas at San Antonio, San Antonio, Texas, USA
[5]Department of Physics and Astronomy, University of Iowa, Iowa City, Iowa, USA
[6]NASA Goddard Space Flight Center, Greenbelt, Maryland, USA
[7]Space Research Corporation, Annapolis, Maryland, USA
[8]Laboratory for Atmospheric and Space Physics, University of Colorado, Boulder, Colorado, USA

Key Points:

- Our model illustrates the structure and state of Ganymede's magnetosphere during Juno's flyby.
- Juno did not enter the closed field line region unless the plasma pressure was exceptionally low.
- We estimate the location of the open-closed-field line-boundary and consider model uncertainties.

Corresponding author: Stefan Duling, `stefan.duling@uni-koeln.de`,
`https://orcid.org/0000-0001-7220-9610`

Abstract

On June 7th, 2021 the Juno spacecraft visited Ganymede and provided the first in situ observations since Galileo's last flyby in 2000. The measurements obtained along a one-dimensional trajectory can be brought into global context with the help of three-dimensional magnetospheric models. Here we apply the magnetohydrodynamic model of Duling et al. (2014) to conditions during the Juno flyby. In addition to the global distribution of plasma variables we provide mapping of Juno's position along magnetic field lines, Juno's distance from closed field lines and detailed information about the magnetic field's topology such as the boundary between open and closed field lines on Ganymede's surface. To estimate the sensitivity of the model results, we carry out a parameter study with different upstream plasma conditions and other model parameters. Utilizing auroral observations by Juno our model indicates that Juno did not enter the closed field line region unless the plasma pressure was exceptionally low.

Plain Language Summary

In June 2021 the Juno spacecraft flew close to Ganymede, the largest moon of Jupiter, and explored it's magnetic and plasma environment. Ganymede's own magnetic field forms a magnetosphere, which is embedded in Jupiter's large-scale magnetic field, and which is unique in the solar system. The vicinity of Ganymede is separated into regions that differ in whether the magnetic field lines connect to Ganymede's surface or not. These regions are deformed by the plasma flow and determine the state of the plasma and the location of Ganymede's aurora. We perform simulations of the plasma flow and interaction to reveal the three-dimensional structure of Ganymede's magnetosphere during the flyby of Juno. Considering possible values for unknown model parameters, we also estimate the uncertainty of the model results. The model provides the three-dimensional state of the plasma and magnetic field, predicted locations of the aurora and the geometrical magnetic context for Juno's trajectory. We find that Juno most likely did not cross the region with field lines that connect to Ganymede's surface at both ends.

1 Introduction

As the largest moon in the solar system, Ganymede not only resides inside Jupiter's huge magnetosphere but also possesses an intrinsic dynamo magnetic field (M. G. Kivelson et al., 1996). The co-rotating Jovian plasma overtakes Ganymede in its orbit with sub-alfvénic velocity and drives an interaction that is unique in the solar system. The internal field acts as an obstacle for the incoming plasma flow, generating plasma waves and electric currents along the magnetopause and emerging Alfvén wings (Gurnett et al., 1996; Frank et al., 1997; Williams et al., 1997). The incoming Jovian magnetic field reconnects at the boundary of a donut-shaped equatorial volume of closed field lines that are defined by both ends connecting to Ganymede's surface (M. G. Kivelson et al., 1997). The open field lines in the polar regions connect to Jupiter at the other end and define the extent of Ganymede's magnetosphere. Near the open-closed-field line-boundary (OCFB) on Ganymede's surface observations by Hubble Space Telescope revealed the presence of two auroral ovals (Hall et al., 1998; Feldman et al., 2000).

Juno's flyby on June 7th, 2021 provided the first in situ measurements of Ganymede's environment, surface and interior since the last Galileo flyby 20 years ago. By approaching Ganymede from the downstream side, Juno crossed the magnetospheric tail for the first time. Juno encountered Ganymede with a minimum distance of ∼0.4 radii (1046km) on a trajectory heading northwards and towards Jupiter, leaving the interaction system at its flank (Hansen et al., 2022).

For analyzing and interpreting the measurements obtained by Juno (Allegrini et al., 2022; Clark et al., 2022; Kurth et al., 2022) it is beneficial to look at its trajectory

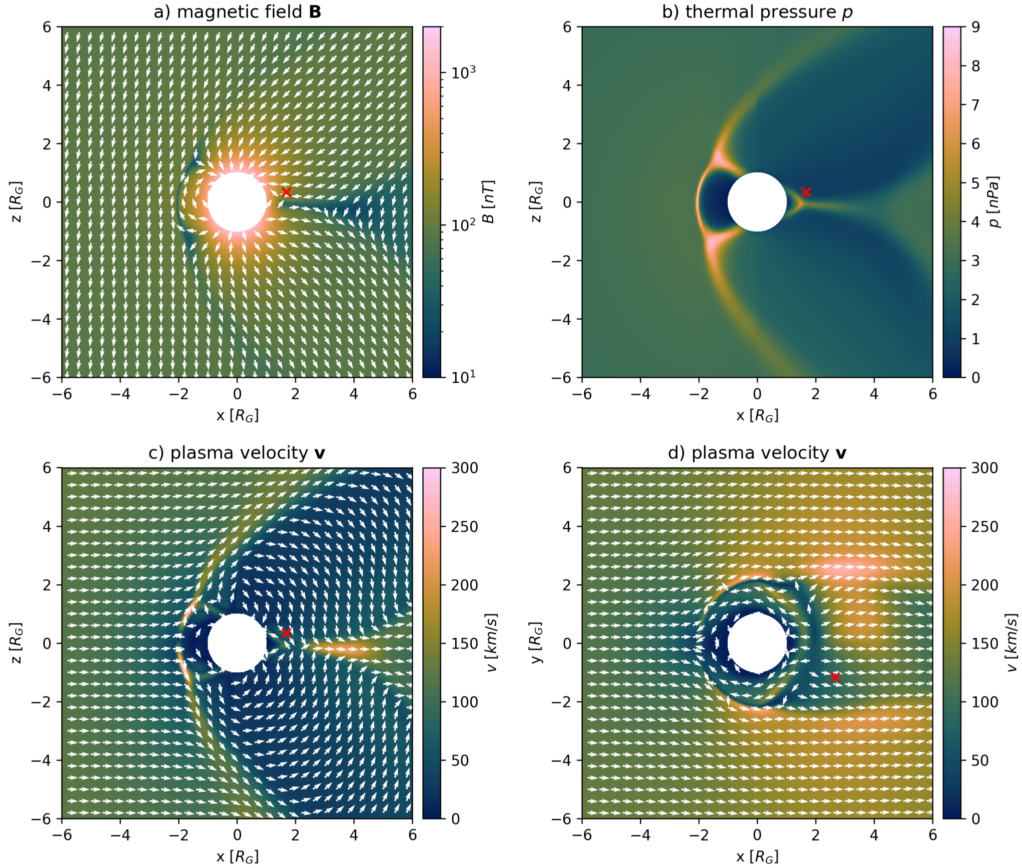

Figure 1. Selected model variables on selected planes, plasma flow from left to right. As seen in direction of Jupiter, y=0 plane: a) Magnetic field B, b) thermal pressure p, c) velocity v. Equatorial plane, as seen from the north, z=0: d) velocity v. The red crosses indicate Juno's crossing through these planes.

with respect to magnetospheric geometries and properties. Instrument data alone cannot uniquely conclude whether Juno crossed the closed field line region. Related to this is the question where observed particles interact with Ganymede's surface, i.e. where Juno's magnetic footprint was located. Furthermore, Juno's UVS instrument provided auroral images at unprecedented resolution (Greathouse et al., 2022). Since electron acceleration processes driving Ganymede's aurora are not yet fully understood, the relation of observed aurora location and magnetic topology are of considerable interest. The aim of this work is thus to provide field and mapping properties during the flyby and illustrate the three-dimensional context of Juno's measurements.

2 Model

We describe Ganymede's space environment by adopting a magnetohydrodynamic (MHD) model based on Duling et al. (2014), which describes a steady state solution for a fixed position in Jupiter's magnetosphere. In our single-fluid approach the plasma interaction is described by the plasma mass density ρ, plasma bulk velocity $\mathbf{v}$, total thermal pressure p and the magnetic field $\mathbf{B}$. For these variables appropriate boundary conditions are applied at Ganymede's surface and a distance of 70 Ganymede radii (R_G).

Our model features simplified photo-ionization, elastic collisions with an O_2 atmosphere and recombination. Ganymede's intrinsic magnetic field is described by dipole Gauss coefficients $g_1^0 = -716.8$ nT, $g_1^1 = 49.3$ nT, $h_1^1 = 22.2$ nT (M. Kivelson et al., 2002). During Juno's visit Ganymede was near the center of the current sheet where the induction response of an expected ocean (Saur et al., 2013) is close to minimum. In our model the induced field has a maximum surface strength of 15.6 nT. The upstream plasma conditions are adjusted to the flyby situation as discussed in Section 4.1. They characterize the interaction to be sub-Alfvénic with an Alfvén Mach number of 0.8 and a plasma beta of 1.1.

While we utilized the ZEUS-MP code (Hayes et al., 2006) in Duling et al. (2014) we now present results obtained with the PLUTO code (Mignone et al., 2007). In Section 4 we validate our results by comparing the outcome of both codes and further analyze the model sensitivity on parameter uncertainties. A detailed description of our model (S1) and its numerical implementation (S2) is attached in the Supplementary Information. For presenting results we use the GPhiO coordinates, where the primary direction z is parallel to Jupiter's rotation axis, the secondary direction y is pointing towards Jupiter and x completes the right-handed system in direction of plasma flow.

3 Results

For the time of closest approach (CA) the Jovian background magnetic field was inclined by $\sim 20°$ to Ganymede's spin axis and approximately aligned to Ganymede's dipole axis, leading to a sub-alfvénic interaction that is nearly symmetric to the $y = 0$ plane. Ganymede's magnetosphere is characterized by northern and southern Alfvén wings, both bent in the orbital direction by $\sim 45°$. In Figure 1 these can be identified by a tilted magnetic field and lowered plasma velocity and pressure. Inside the Alfvén wings the plasma velocity is reduced below 50 km/s. The convection through the wings over the poles is slowed down and takes about 10 minutes for a distance of 10 R_G. Additionally, the interaction expands the volume characterized by closed field lines on the upstream side while it is strongly compressed on the downstream side. This area has a thermal pressure below 1 nPa in Figure 1b. The diameter of Ganymede's magnetosphere is about 4 R_G in the equatorial plane as indicated by the reduced velocity in Figure 1d. On the downstream side the reduced velocity also indicates a stretched magnetospheric tail with more than 10 R_G length that was crossed by Juno at the location of the red cross.

3.1 Magnetic Topology

In Figure 2 and Movie S3, we display the modeled magnetic field topology together with Juno's trajectory. The punctures of the red line through the blue surface indicate where Juno entered and left the volume with open field lines, i.e. Ganymede's magnetosphere. In our model the crossings occurred inbound at 16:49:25 on the tail side and at 17:00:25 outbound at the northern Jupiter-facing side. We do not see Juno on closed field lines at any time. The height of the closed field line region, green in Figure 2, increases in upstream direction. Juno's trajectory is located slightly above this boundary and inclined by a similar angle. Therefore the closest distance between Juno and closed field lines was nearly constant below 0.2 R_G for about 6 minutes, with two minima of ~ 0.013 R_G at the time of CA and the outbound crossing (Figure 4).

The modeled location of the OCFB on the surface of Ganymede is shown in Figure 3 as two green lines. The plasma flow generates magnetic stresses which push the OCFB ovals pole-wards on the upstream side and presses them together on the downstream side. Here the averaged latitude (between 45° and 135° W) is at 27.5° (north) respectively -30.8° (south). Figure 3 also shows results from simulations with the background field before (dotted) and after (dashed) the flyby; the OCFB ovals appear to migrate in opposite directions, west for the northern and east for the southern oval. In latitudinal

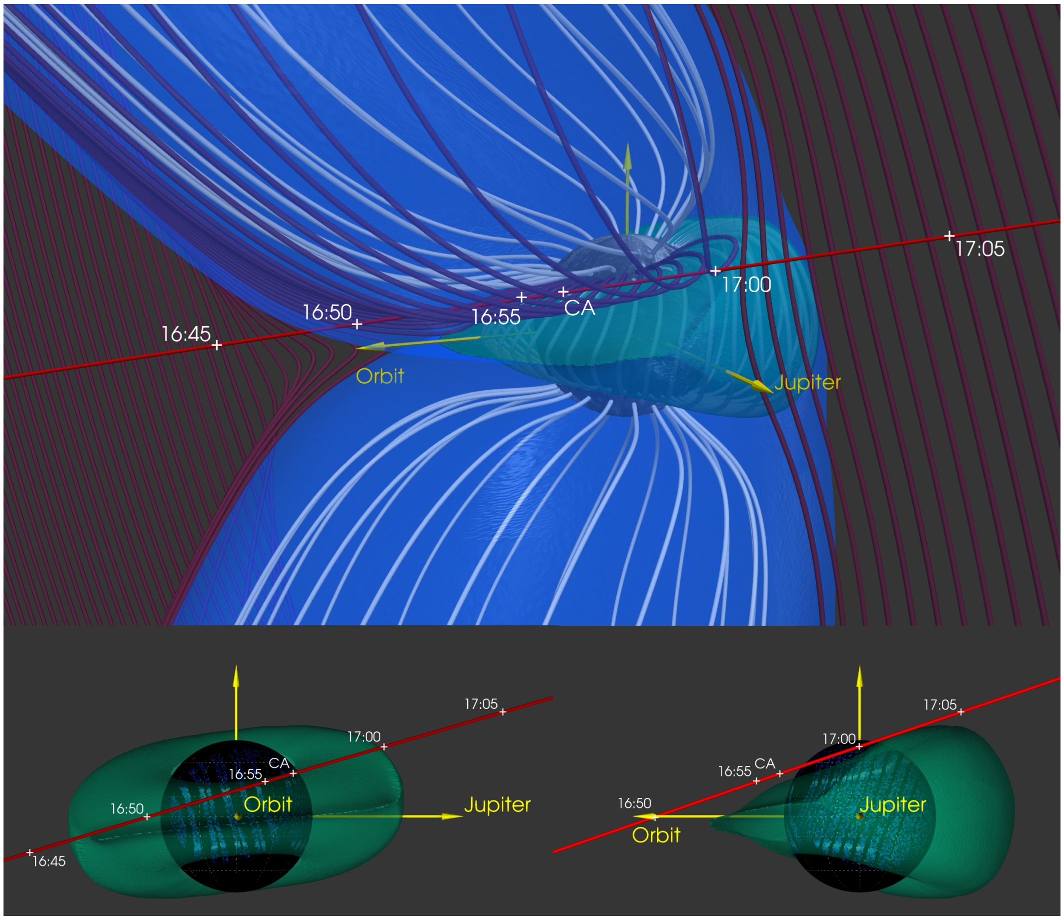

Figure 2. Juno's trajectory (red) in relation to the modeled magnetosphere during the flyby of Ganymede. The timestamps in UTC indicate the position of Juno. In the upper panel the tubes show selected magnetic field lines connected to Ganymede's surface (white) and Juno's trajectory (dark). The green surface represents the outer boundary of closed field lines, the blue surface represents the outer boundary of open field lines that connect to Ganymede at one end. The bottom panel additionally shows observed 130.4 and 135.6 nm oxygen emissions from the aurora (Greathouse et al., 2022).

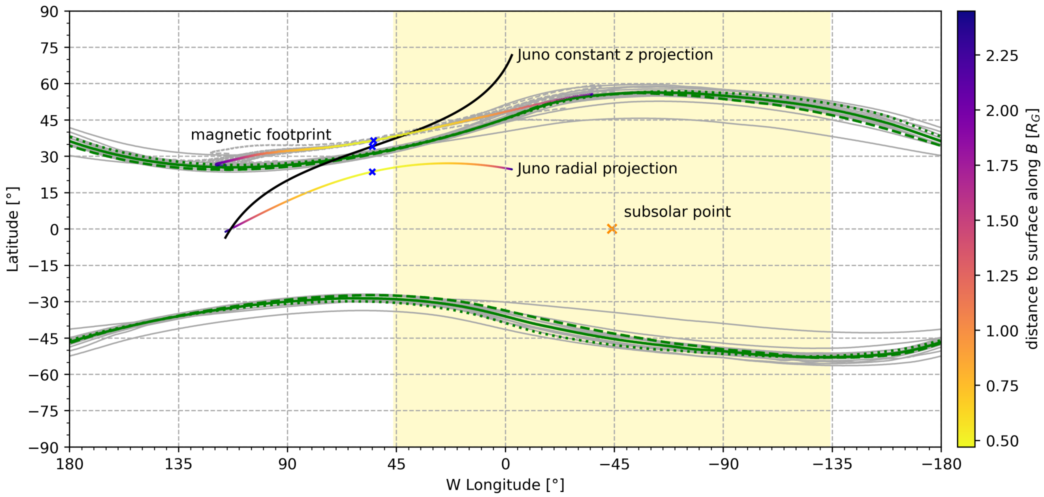

Figure 3. Surface map of Ganymede with 0° western longitude pointing towards Jupiter (GPhiO). The modeled OCFB for the time of CA is shown as green lines. The dotted (dashed) lines show its location based on the measured background field before (after) the flyby. Juno's position is projected in radial direction and shown as the lower multicolored line, the same with constant z as black line. The upper multicolored line shows the location where field lines end that are connected to Juno, namely Juno's magnetic footprint. Color coded is the distance along those field lines. The blue crosses mark the locations at CA. The area that was illuminated by the sun is shown in yellow, neglecting an inclination of 0.2°; the sub-solar point as orange cross. The faint gray lines indicate the model uncertainty due to the inaccurate knowledge of upstream plasma conditions and other model parameters (Section 4).

direction the highest sensitivity to the background field occurs at the flanks of the magnetosphere. While Juno was outside closed field lines, its radially projected position was within the OCFB ovals for the complete stay inside the magnetosphere. In Figure 3 this is shown by the lower multicolored line with its endpoints referring to the magnetopause crossings. They also correspond to the vertical lines in Figure 4 and the surface punctures in Figure 2. Mapping the field lines from Juno's position to the surface yields its magnetic footprint, as shown as upper multicolored line in Figure 3. Since the colors indicate the lengths of the field lines between Juno and the surface, the footprint location associated with the position of the spacecraft can be identified by a shared color. Juno's footprint is modeled to be up to 6° and on average 4° degree north of the OCFB. Before CA Juno's position maps to nearly the same meridian on the surface. After CA the field lines become more bent in longitudinal direction (Figure 2) resulting in an eastern shift of Juno's footprint. Juno's footprint touches the OCFB at both ends. While this is counter intuitive at first glance, it is a direct consequence of the magnetic topology. Every magnetopause crossing, although possibly far away from closed field lines, touches an outermost open field line that maps to the OCFB at the surface. This convergence of field lines brings the footprints on the surface closer to the OCFB than Juno's position itself.

3.2 Comparison with Magnetometer Measurements

In Figure 4 we compare modeled magnetic field with magnetometer measurements (Connerney et al., 2017) along Juno's trajectory. The vertical lines represent the modeled times when Juno entered and left the open field line region, namely the inbound and outbound magnetopause crossings. Although short-term fluctuations are not covered by

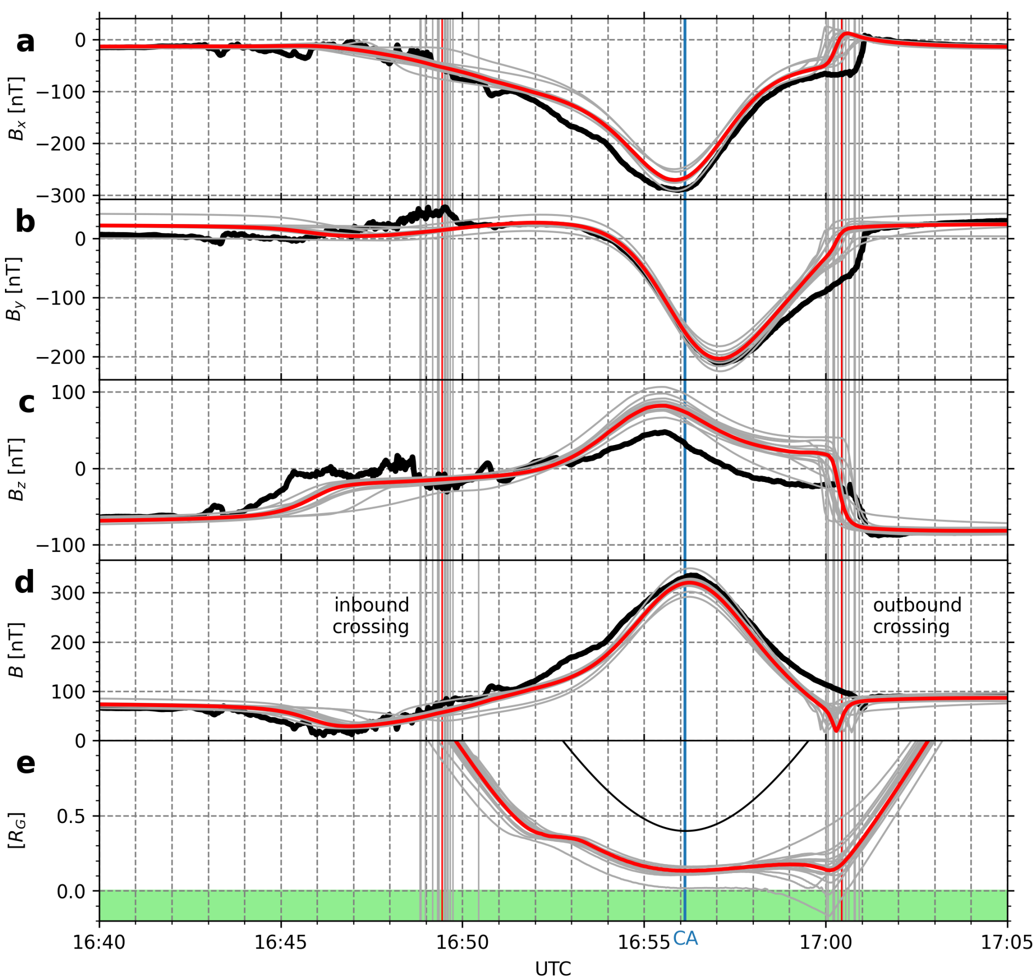

Figure 4. Modeled (red) versus measured (black) magnetic field along Juno's trajectory. Panels a-c show GPhiO components, panel d the magnitude. Panel e shows Juno's distance from Ganymede's surface (black) and the OCFB (red) in R_G, with negative values (green) indicating locations inside the closed field line region. The vertical lines represent the modeled inbound and outbound magnetopause crossings. The faint gray lines indicate the model uncertainty due to the uncertain knowledge of upstream conditions and other model parameters (Section 4).

our model, it reproduces the field rotations and overall structure very well. We identify three noticeable deviations. (1) At CA B_x and the magnitude are underestimated by $\sim$20 nT. (2) In the closer vicinity of Ganymede B_z is underestimated by $\sim$35 nT. These two deviations might indicate an inaccurate model of the intrinsic field. (3) The model features a clear outbound crossing but it is located slightly too far inwards and occurs $\sim$30 s too early. Inaccurate upstream conditions might be the reason for this (Section 4.2). During the inbound crossing, however, both the measurements and our model do not indicate a rotation.

4 Model Robustness

For the interpretation of Juno's measurements a model can play an important role. In contrast to measurements it is not feasible to apply a detailed error analysis to assess the uncertainty of our results. However, to estimate the numerical error, we utilize a second independent simulation code with different solver algorithms. Using the ZEUS code, the OCFB is identically within 0.5° latitude (downstream) and 2° (upstream) (Table 1). The magnetosphere has a similar shape, predicting the magnetopause crossings 25s earlier and Juno outside of closed field lines with a sharp minimal distance of 0.02 R_G at Ganymede's flank. Further inaccuracies are consequences of unknown or uncertain physical parameters and upstream conditions, which are addressed in detail in the remainder of this section.

4.1 Uncertainty Range of Model Parameters

Our model uses homogeneous and steady-state upstream conditions. An appropriate value for the Jovian magnetic field can directly be obtained from measurements of the magnetometer on-board Juno. Therefore the undisturbed field measurements before ((-16,3,-70) nT) and after ((-14,43,-80) nT) the flyby (Weber et al., 2022) have to be interpolated to receive a value suitable for the situation during CA ((-15,24,-75) nT). This value has some uncertainties because the temporal change is possibly non-linear and the convection time might play a role as well. The measurements before and after CA are nevertheless upper and lower limits for the magnetic field.

Upstream plasma conditions are more difficult to determine. Juno's JADE and JEDI instruments provide particle distribution functions which in theory enable numerical moment calculations to achieve the plasma density, velocity and thermal pressure. However, at the moment numerical moments do not provide reliable values. Until refined analysis might help to determine those upstream conditions in the future, we access predictions. The plasma velocity relative to Ganymede depends on how strongly Jupiter's magnetosphere sub-corotated during the flyby. Voyager and Galileo data suggest a relative velocity of 140 km/s with a variability of 20 km/s (M. G. Kivelson et al., 2022). The density is expected to vary by a factor of 5 depending on Ganymede's position with respect to the current sheet (Jia et al., 2008), whereas literature values reveal larger uncertainties: 54 amu/cm^3 on average with a variability of 2-100 amu/cm^3 (M. G. Kivelson et al., 2004), 30 (13-46) amu/cm^3 with an uncertainty factor of 2 (Bagenal & Delamere, 2011), 160 amu/cm^3 inside the current sheet and 48 amu/cm^3 on higher magnetic latitudes (M. G. Kivelson et al., 2022). JADE measured 1 /cm^3 protons and 8 /cm^3 heavy ions before the flyby (Allegrini et al., 2022), consistent with electron densities of 5-12 /cm^3 observed by the Waves instrument outside of the magnetosphere (Kurth et al., 2022). We assume 100 amu/cm^3 for our model and investigate the effects of extreme densities 10 and 160 amu/cm^3. The thermal pressure is dominated by energetic particles in the vicinity of Ganymede (Mauk, 2004). Therefore JEDI measurements provide a lower limit to the pressure during the flyby Clark et al. (2022), calculating 1.5 nPa for the >50 keV protons. Sulfur and oxygen are expected to have a significant but unknown contribution. Former models assumed 3.8 nPa (Jia et al., 2008; Duling et al., 2014), here we use 2.8 nPa as also spec-

Table 1. Variations of model parameters and upstream conditions and their effect on presented model results. Columns 3-6 specify the averaged latitude of the northern and southern open closed field line boundary (OCFB) on Ganymede's surface on the upstream (-45° to -135°W) and downstream (45° to 135°W) side. Column 7 states Juno's closest distance to closed field lines and columns 8-9 the UTC times of its inbound respectively outbound magnetopause crossings.

		OCFB down		OCFB up		dist. to	magnetopause crossing	
parameter	value	N [°]	S [°]	N [°]	S [°]	CF [R_G]	inbound	outbound
default model	- [a]	27.5	-30.8	54.3	-50.2	0.13	16:49:25	17:00:25
default model	ZEUS code	28.1	-31.2	56.4	-51.8	0.02	16:48:50	17:00:00
B_0 before CA	(-16,3,-70) nT [d]	28.3	-31.6	55.5	-51.1	0.13	16:49:34	17:00:54
B_0 after CA	(-14,43,-80) nT [d]	26.9	-30.0	53.1	-49.2	0.11	16:49:29	17:00:03
velocity	120 km/s [e]	27.5	-30.9	52.7	-48.5	0.13	16:49:35	17:00:25
velocity	160 km/s [e]	27.7	-30.8	55.6	-51.7	0.05	16:49:19	17:00:27
density	10 amu/cm^3 [f]	28.5	-32.3	43.3	-38.9	0.10	16:50:26	17:00:46
density	160 amu/cm^3 [e]	28.0	-31.0	56.7	-52.9	0.00[b]	16:49:18	17:00:27
pressure	1 nPa	32.7	-35.9	57.3	-53.2	0.00[c]	16:48:58	17:00:48
pressure	5 nPa	26.5	-29.8	53.3	-49.2	0.15	16:49:43	17:00:11
production	0.5e-8 /s	27.3	-30.5	54.3	-50.2	0.14	16:49:31	17:00:26
production	10e-8 /s	27.5	-30.7	52.9	-48.9	0.13	16:49:10	17:00:26
atmosphere	1.6e6 /cm^3	27.7	-30.9	54.7	-50.5	0.11	16:49:39	17:00:32
atmosphere	40e6 /cm^3	28.4	-31.9	50.6	-46.6	0.12	16:48:49	17:00:19
dynamo g_1^0	-10%	25.8	-29.3	53.6	-49.2	0.16	16:49:30	17:00:13
dynamo g_1^0	+10%	29.1	-32.1	55.0	-51.1	0.10	16:49:20	17:00:37

[a]: default values: (-15,24,-75) nT [d], 140 km/s [e], 100 amu/cm^3, 2.8 nPa [e], 2.2e.8 /s, 8e6 /cm^3
[b]: Juno was on closed field lines between 16:59:55 and 17:00:11.
[c]: Juno was on closed field lines between 16:58:25 and 17:00:34.
[d]: Weber et al. (2022)
[e]: M. G. Kivelson et al. (2022)
[f]: Bagenal and Delamere (2011)

ified by M. G. Kivelson et al. (2022) and consider generous limits of 1.0 nPa and 5.0 nPa as uncertainties.

The dominating primary dipole moment g_1^0 of Ganymede's dynamo field is determined from 3 Galileo flybys with an uncertainty of less than 3% (M. Kivelson et al., 2002). We cover a larger uncertainty by considering a variation of 10%. Further, we investigate the model's sensitivity to our parametrization of the atmosphere and photo-ionization as these effects determine the plasma state inside Ganymede's magnetosphere. We assume uncertainties of the atmosphere's surface density and the plasma production rate varying by a factor of 5.

4.2 Model Sensitivities on Parameter Uncertainties

The considered parameter variations change the size and shape of the magnetosphere differently. Table 1 summarizes the sensitivities of important model results to different parameter variations. A significantly later outbound magnetopause crossing (17:00:54 latest) is modeled only if the upstream plasma density or pressure is extraordinary low or the measured background field before CA is used. The latter is unlikely to still represent the background field when Juno crossed the magnetopause about 5 minutes after passing CA. With an uncertainty of ∼1.5 minutes the inbound crossing is by a factor of two more sensitive than the outbound crossing (∼45 seconds), as expected from the more dynamic tail where Juno entered Ganymede's magnetosphere. Here the strongest variations are caused by a more dense atmosphere and a low pressure (each 30 seconds earlier). In contrast to the outbound crossing a low plasma density affects the inbound crossing (1 minute later) in the opposite sense.

Within realistic ranges the plasma pressure is the parameter that mostly affects the size of the magnetosphere. The lowest assumed pressure inflates the complete magnetosphere resulting in a pole-wards shift of the OCFB by 3-5°. In Figure 3 the sensitivity of the OCFB is indicated by the gray lines, each representing one of the listed parameter variations. In general its upstream location is more sensitive to changing upstream conditions than on the downstream side. Neglecting special cases of lower pressure (downstream) and low density (upstream) the modeled surface OCFB has an uncertainty of ∼3° (downstream) respectively ∼6.5° (upstream). On the downstream side, the most equator-wards shift of the OCFB is achieved from a higher pressure and values 1° or up to 2° if the dynamo strength is lowered by 10%.

The sensitivity of Juno's distance to closed field lines can also be inferred from the gray lines in Figure 4. As already shown by the surface OCFB locations a lower than expected plasma pressure increases the size of the magnetosphere and therefore directly affects the distance between Juno's trajectory and closed field lines. In case of 1 nPa Juno possibly entered closed field line regions for more than 2 minutes between 16:58:25 and 17:00:34. Juno would also have been on closed field lines with using a higher density of 160 amu/cm^3 although the corresponding time window lasted only 16 seconds just before leaving the magnetosphere. As Figure 4 suggests, the sensitivity of the distance to closed field lines to parameters beside pressure can be divided into two parts. Before ∼16:58 the uncertainty is quite constant $<0.05\ R_G$. After ∼16:58, around the outbound crossing, when Juno was above the flank of the closed field line region, the uncertainty is larger and several parameter variations significantly reduce the distance (cf. Table 1). If Juno crossed closed field lines, it was most likely in this region. The more dynamic character of the flank is also visible at the increased sensitivity of the OCFB around 0° in Figure 3.

5 Discussion

We performed MHD simulations of Ganymede's magnetosphere which put Juno's observations into a three-dimensional context. Our results help to answer questions that arise from analyzing the measurements. Model uncertainties are assessed through a sensitivity study to uncertain upstream conditions.

The question of whether Juno was on closed field lines or not is determined by the geometrical shape of Ganymede's magnetosphere. The times of measured magnetopause crossings by Juno provide strong geometrical constraints for magnetospheric models. The various instruments onboard Juno detected the outbound crossing more clearly than the inbound, matching expectations of a more dynamic magnetotail. Our model predicts that Juno left Ganymede's magnetosphere at 17:00:25, 5s earlier than JEDI (Clark et al., 2022), 12s earlier than JADE (Allegrini et al., 2022) and about 30s earlier than MAG (Romanelli et al., 2022) and the Waves instrument (Kurth et al., 2022) identified the outbound crossing. Additionally we can use aurora locations as observed by Juno's UVS (Greathouse et al., 2022) to further constrain the modeled geometry. Although auroral electron acceleration mechanisms are not fully understood, the observed sharp pole-ward decay of the auroral emission suggests a correlation of the surface OCFB and the auroral edges. Therefore we consider the outbound magnetopause crossing and the observed aurora as two main constraints to evaluate the geometrical quality of our model. Despite uncertainty ranges of upstream conditions and model parameters have been examined our model does not fit both constraints equally well. In fact we even detect an opposing behaviour. Parameter variations fitting the aurora better lead to a worse fit to the outbound crossing.

However, since the aurora was observed ∼4° (north) respectively ∼5° (south) more equatorial between 0°W and 135°W (Greathouse et al., 2022) it seems that our model slightly overestimates the north-south extent of the volume with closed field lines on the downstream side (cf. Figure 2). In general this extent is not expected to increase with distance from the surface. Juno's position though, projected with constant z to the surface is already located north of the modeled surface OCFB for the close-by parts of the flyby (cf. Figure 3). Taking into account that the observed aurora suggests a thinner volume with closed field lines it appears very unlikely that Juno was on closed field lines during its flyby on June 7th, 2021.

Acknowledgments

This project has received funding from the European Research Council (ERC) under the European Union's Horizon 2020 research and innovation programme (Grant agreement No. 884711). The research at the University of Iowa is supported by NASA through Contract 699041X with Southwest Research Institute. The MHD simulation codes utilized for this work are open-source projects. PLUTO can be downloaded at http://plutocode.ph.unito.it/ (version 4.4). ZEUS-MP is available at http://www.netpurgatory.com/zeusmp.html (version 2.1.2). The numerical simulations have been performed on the CHEOPS Cluster of the University of Cologne, Germany. Juno MAG data are publicly available through the Planetary Data System (https://pds-ppi.igpp.ucla.edu/) at https://doi.org/10.17189/1519711.

References

Allegrini, F., Bagenal, F., Ebert, R., Louarn, P., McComas, D. J., Szalay, J., . . . Waite, J. H. (2022). Plasma observations during the june 7, 2021 ganymede flyby from the jovianauroral distributions experiment (jade) on juno. *Geophysical Research Letters*, *this issue*.

Bagenal, F., & Delamere, P. A. (2011, may). Flow of mass and energy in the magnetospheres of jupiter and saturn. *Journal of Geophysical Research: Space Physics*, *116*(A5). doi: 10.1029/2010ja016294

Clark, G., Mauk, B. H., Paranicas, C., Kollmann, P., Haggerty, D., Rymer, A., . . . Turner, D. L. (2022). Energetic charged particle observations during juno's close flyby of ganymede. *Geophysical Research Letters*, *this issue*.

Connerney, J. E. P., Benn, M., Bjarno, J. B., Denver, T., Espley, J., Jorgensen, J. L., . . . Smith, E. J. (2017, feb). The juno magnetic field investigation. *Space Science Reviews*, *213*(1-4), 39–138. doi: 10.1007/s11214-017-0334-z

Duling, S., Saur, J., & Wicht, J. (2014, jun). Consistent boundary conditions at nonconducting surfaces of planetary bodies: Applications in a new ganymede MHD model. *Journal of Geophysical Research: Space Physics*, *119*(6), 4412–4440. doi: 10.1002/2013ja019554

Feldman, P. D., McGrath, M. A., Strobel, D. F., Moos, H. W., Retherford, K. D., & Wolven, B. C. (2000, jun). HST/STIS ultraviolet imaging of polar aurora on ganymede. *The Astrophysical Journal*, *535*(2), 1085–1090. doi: 10.1086/308889

Frank, L. A., Paterson, W. R., Ackerson, K. L., & Bolton, S. J. (1997, sep). Low-energy electron measurements at ganymede with the galileo spacecraft: Probes of the magnetic topology. *Geophysical Research Letters*, *24*(17), 2159–2162. doi: 10.1029/97gl01632

Greathouse, T. K., Gladstone, R., Molyneux, P. M., Versteeg, M. H., Hue, V., Kammer, J., . . . Duling, S. (2022). Uvs observations of ganymede's aurora during juno orbits 34 and 35. *Geophysical Research Letters*, *this issue*.

Gurnett, D. A., Kurth, W. S., Roux, A., Bolton, S. J., & Kennel, C. F. (1996, dec). Evidence for a magnetosphere at ganymede from plasma-wave observations by the galileo spacecraft. *Nature*, *384*(6609), 535–537. doi: 10.1038/384535a0

Hall, D. T., Feldman, P. D., McGrath, M. A., & Strobel, D. F. (1998, may). The far-ultraviolet oxygen airglow of europa and ganymede. *The Astrophysical Journal*, *499*(1), 475–481. doi: 10.1086/305604

Hansen, C. J., Bolton, S., Sulaiman, A., Duling, S., Brennan, M., Connerney, J., ... Withers, P. (2022). Juno's close encounter with ganymede - an overview. *Geophysical Research Letters*, *this issue*.

Hayes, J. C., Norman, M. L., Fiedler, R. A., Bordner, J. O., Li, P. S., Clark, S. E., ... Low, M.-M. M. (2006, jul). Simulating radiating and magnetized flows in multiple dimensions with ZEUS-MP. *The Astrophysical Journal Supplement Series*, *165*(1), 188–228. doi: 10.1086/504594

Jia, X., Walker, R. J., Kivelson, M. G., Khurana, K. K., & Linker, J. A. (2008, jun). Three-dimensional MHD simulations of ganymede's magnetosphere. *Journal of Geophysical Research: Space Physics*, *113*(A6), n/a–n/a. doi: 10.1029/2007ja012748

Kivelson, M., Khurana, K., & Volwerk, M. (2002, jun). The permanent and inductive magnetic moments of ganymede. *Icarus*, *157*(2), 507–522. doi: 10.1006/icar.2002.6834

Kivelson, M. G., Bagenal, F., Jia, X., Khurana, K., Volwerk, M., & Zarka, P. (2022). Ganymede's magnetosphere and its interaction with the jovian magnetosphere. In M. Volwerk & M. McGrath (Eds.), *Ganymede.* Cambridge, UK: Cambridge University Press.

Kivelson, M. G., Bagenal, F., Kurth, W. S., Neubauer, F. M., Paranicas, C., & Saur, J. (2004). Magnetispheric interaction with satellites. In *Jupiter - the planet, satellites and magnetosphere* (p. 513-536). Cambridge Univ. Press, New York.

Kivelson, M. G., Khurana, K. K., Coroniti, F. V., Joy, S., Russell, C. T., Walker, R. J., ... Polanskey, C. (1997, sep). The magnetic field and magnetosphere of ganymede. *Geophysical Research Letters*, *24*(17), 2155–2158. doi: 10.1029/97gl02201

Kivelson, M. G., Khurana, K. K., Russell, C. T., Walker, R. J., Warnecke, J., Coroniti, F. V., ... Schubert, G. (1996, dec). Discovery of ganymede's magnetic field by the galileo spacecraft. *Nature*, *384*(6609), 537–541. doi: 10.1038/384537a0

Kurth, W., Sulaiman, A., Hospodarsky, G. B., Menietti, J., Mauk, B. H., Clark, G., ... Louis, C. (2022). Juno plasma wave observations at ganymede. *Geophysical Research Letters*, *this issue*.

Marconi, M. (2007, sep). A kinetic model of ganymede's atmosphere. *Icarus*, *190*(1), 155–174. doi: 10.1016/j.icarus.2007.02.016

Mauk, B. H. (2004). Energetic ion characteristics and neutral gas interactions in jupiter's magnetosphere. *Journal of Geophysical Research*, *109*(A9). doi: 10.1029/2003ja010270

Mignone, A., Bodo, G., Massaglia, S., Matsakos, T., Tesileanu, O., Zanni, C., & Ferrari, A. (2007, may). PLUTO: A numerical code for computational astrophysics. *The Astrophysical Journal Supplement Series*, *170*(1), 228–242. doi: 10.1086/513316

Romanelli, N., DiBraccio, G. A., Modolo, R., Connerney, J. E. P., W.Ebert, R., Martos, Y. M., ... Bolton, S. J. (2022). Analysis of juno magnetometer observations:comparisons with a global hybrid simulation andindications of ganymede's magnetopause reconnection. *Geophysical Research Letters*, *this issue*.

Roth, L., Ivchenko, N., Gladstone, G. R., Saur, J., Grodent, D., Bonfond, B., ... Retherford, K. D. (2021, jul). A sublimated water atmosphere on ganymede detected from hubble space telescope observations. *Nature Astronomy*, *5*(10), 1043–1051. doi: 10.1038/s41550-021-01426-9

Saur, J., Grambusch, T., Duling, S., Neubauer, F. M., & Simon, S. (2013, apr). Magnetic energy fluxes in sub-alfvénic planet star and moon planet interactions. *Astronomy & Astrophysics*, *552*, A119. doi: 10.1051/0004-6361/201118179

Weber, T., Moore, K., Connerney, J., Espley, J., DiBraccio, G., & Romanelli, N. (2022). Updated spherical harmonic moments of ganymedefrom the juno flyby. *Geophysical Research Letters*, *this issue*.

Williams, D. J., Mauk, B. H., McEntire, R. W., Roelof, E. C., Armstrong, T. P., Wilken, B., . . . Murphy, N. (1997, sep). Energetic particle signatures at ganymede: Implications for ganymede's magnetic field. *Geophysical Research Letters*, *24*(17), 2163–2166. doi: 10.1029/97gl01931

Figure3.

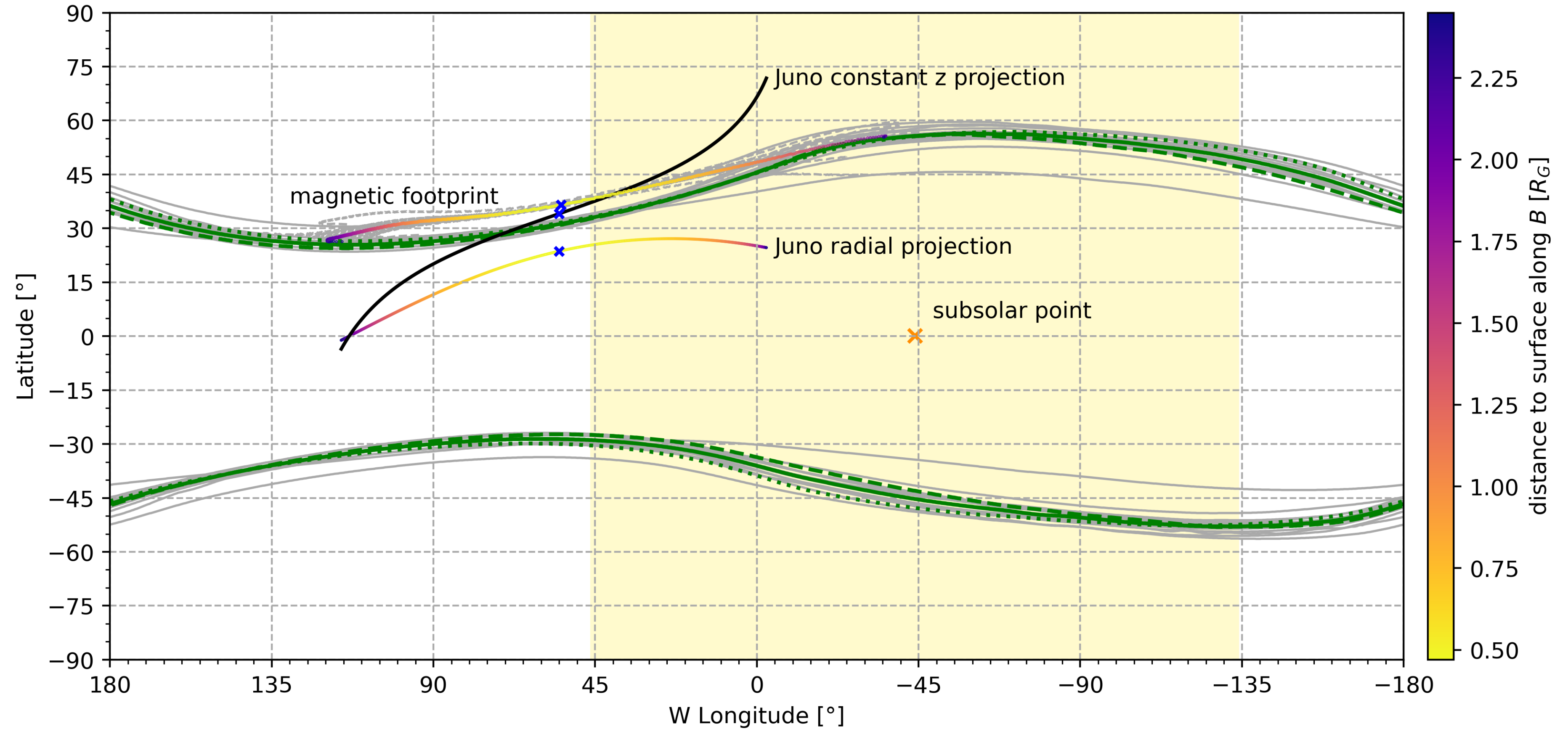

Juno constant z projection
magnetic footprint
Juno radial projection
subsolar point
Latitude [°]
W Longitude [°]
distance to surface along B [R_G]
90
75
60
45
30
15
0
−15
−30
−45
−60
−75
−90
180
135
90
45
0
−45
−90
−135
−180
2.25
2.00
1.75
1.50
1.25
1.00
0.75
0.50

Figure2.

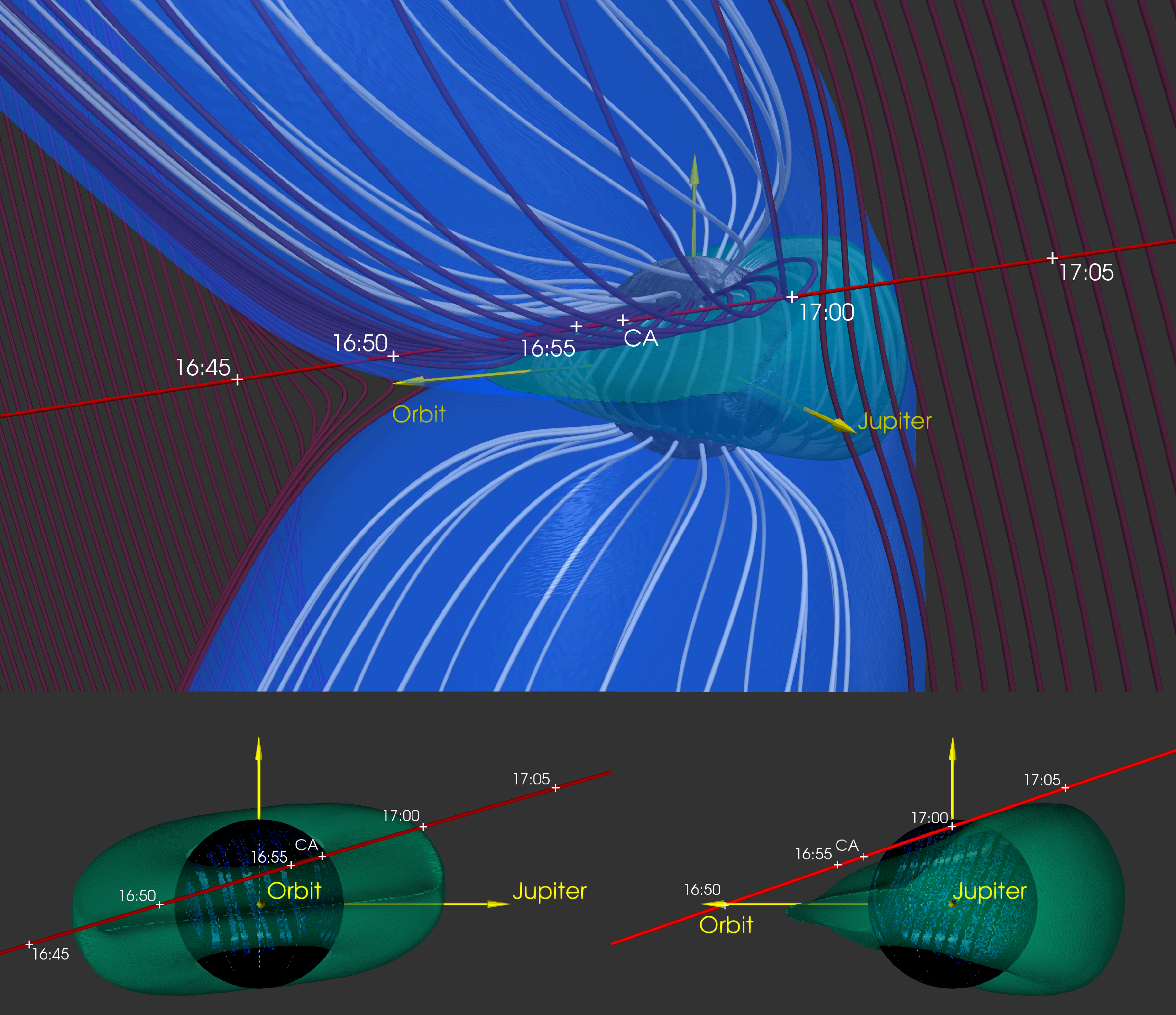
17:05
17:00
CA
16:55
16:50
16:45
Orbit
Jupiter
17:05
17:00
CA
16:55
Orbit
Jupiter
16:50
16:45
17:05
17:00
CA
16:55
16:50
Jupiter
Orbit

Figure4.

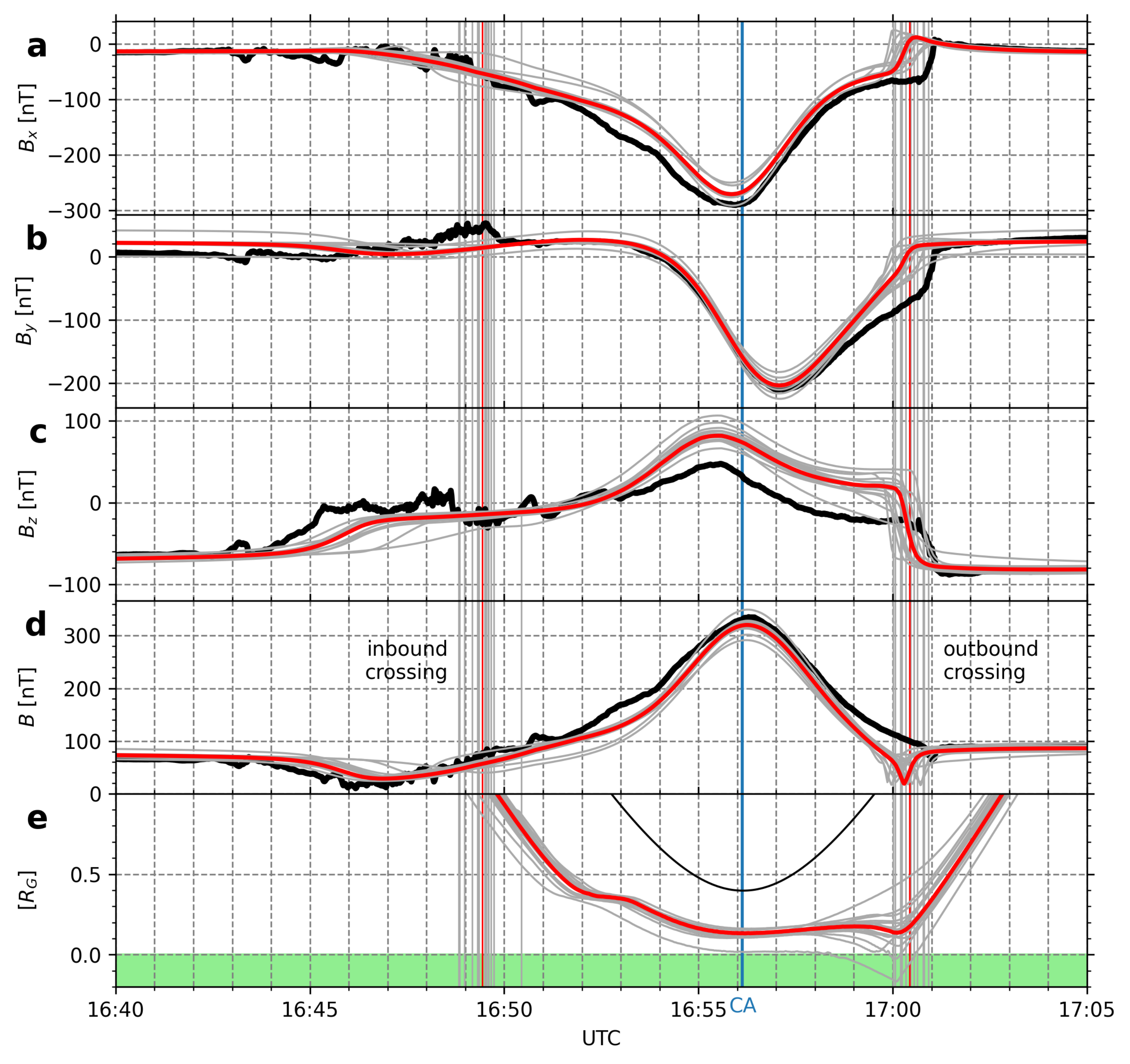

a
b
c
d
e
B_x [nT]
B_y [nT]
B_z [nT]
B [nT]
[R_G]
0
−100
−200
−300
100
inbound crossing
outbound crossing
300
200
0.5
0.0
16:40
16:45
16:50
16:55
CA
17:00
17:05
UTC

Figure1.

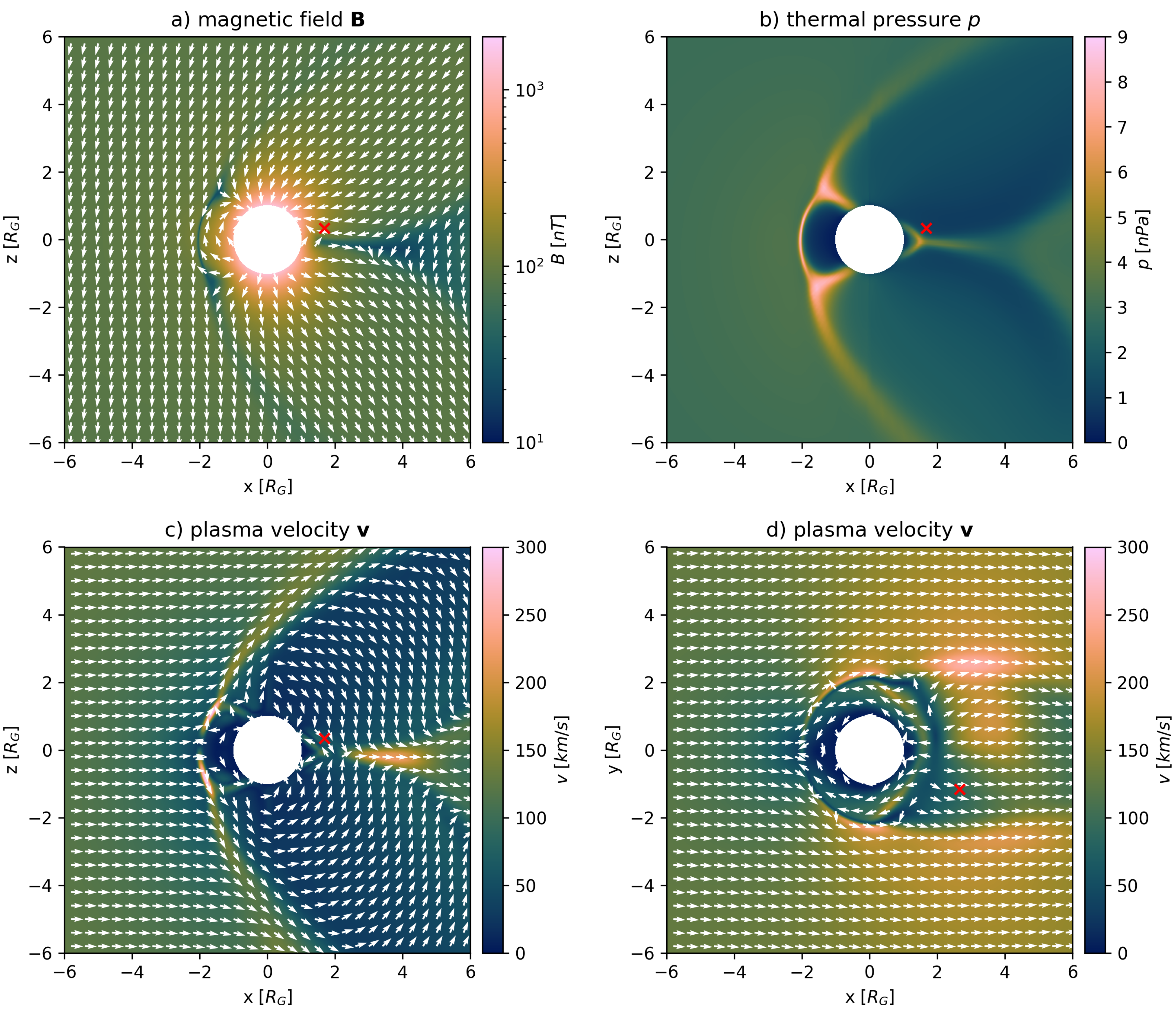
a) magnetic field **B**
b) thermal pressure *p*
c) plasma velocity **v**
d) plasma velocity **v**
z [R_G]
y [R_G]
x [R_G]
B [nT]
p [nPa]
v [km/s]